MPMI Vol. 37, No. 7, 2024, pp. 583–593, https://doi.org/10.1094/MPMI-12-23-0220-R

Small RNA and Degradome Deep Sequencing Reveal Regulatory Roles of MicroRNAs in Response to Sugarcane Mosaic Virus Infection on Two Contrasting Sugarcane Cultivars

Yuan Yuan,[1,2] Cuilin Huang,[1] Kaiyuan Pan,[1] Wei Yao,[1] Rui Xia,[3] and Muqing Zhang[1,†]

[1] State Key Laboratory for Conservation and Utilization of Agro-Bioresources, Guangxi Key Laboratory for Sugarcane Biology, Guangxi University, Nanning 530005, China
[2] Rubber Research Institute, Chinese Academy of Tropical Agricultural Science, Haikou 570105, China
[3] State Key Laboratory for Conservation and Utilization of Subtropical Agro-Bioresources, College of Horticulture, South China Agricultural University, Guangzhou 510642, China

Accepted for publication 8 April 2024.

MicroRNAs (miRNAs) play an essential regulatory role in plant-virus interaction. However, few studies have focused on the roles of miRNAs and their targets after sugarcane mosaic virus (SCMV) infection in sugarcane. To address this issue, we conducted small RNA (sRNA) and degradome sequencing on two contrasting sugarcanes (SCMV-resistant 'Fuoguo1' [FG1] and susceptible 'Badila') infected by SCMV at five time points. A total of 1,578 miRNAs were profiled from 30 sRNA libraries, comprising 660 known miRNAs and 380 novel miRNAs. Differential expression analysis of miRNAs revealed that most were highly expressed during the SCMV exponential phase in Badila at 18 h postinfection, with expression profiles positively correlated with virus replication dynamics as observed through clustering. Analysis of degradome data indicated a higher number of differential miRNA targets in Badila compared to FG1 at 18 h postinfection. Gene ontology (GO) enrichment analysis significantly enriched the stimulus-response pathway, suggesting negative regulatory roles to SCMV resistance. Specifically, miR160 upregulated expression patterns and validated in Badila through quantitative real-time PCR (qRT-PCR) in the early stages of SCMV multiplication. Our research provides new insights into the dynamic response of plant miRNA and virus replication and contributes valuable information on the intricate interplay between miRNAs and SCMV infection dynamics.

Keywords: degradome, miR160, small RNA sequencing, sugarcane, sugarcane mosaic virus

Sugarcane (*Saccharum officinarum* L.) is a significant sugar crop worldwide. Sugarcane mosaic virus (SCMV), a dominant pathogen of sugarcane mosaic disease causing severe economic losses, is a single-stranded sense RNA virus belonging to the genus *Potyvirus*, family Potyviridae (Lakshmanan et al. 2005; Viswanathan and Balamuralikrishnan 2005). SCMV damages cell chloroplasts and reduces photosynthesis, restricting plant growth during viral multiplication (Gao et al. 2011; Xie et al. 2021). During the extensive encounters against viruses, plants have evolved various antiviral mechanisms, of which RNA-silencing-mediated viral resistance is one of the most concerning mechanisms. MicroRNA (miRNA) is an essential small silencing RNA involved in host antimicrobial immunity in eukaryotic organisms (Guo et al. 2019). However, the response of miRNAs for SCMV infection in the early multiplication remains unknown in sugarcane.

Small RNA (sRNA)-mediated silencing was first discovered in plant anti-virus research, which protects the plant immune system against infection, maintains genomic stability, and regulates growth and development (Baulcombe 2004; Ding 2010). sRNA commonly inhibits the expression or translation of target genes by guiding complementary messenger RNA (mRNA) or viral RNA with the degradation, thereby silencing target genes and regulating their expression (Csorba et al. 2009). On the other hand, viruses have evolved RNA-silencing suppressors that affect RNA-induced silencing complex (RISC) assembly and subsequent mRNA degradation in the arms race between plants and viruses, which is for evading the host immune response and

†Corresponding author: M. Q. Zhang; zmuqing@163.com

Author contributions: M.Q.Z. conceived and designed the project. Y.Y. assembled and analyzed the data. C.L.H. performed sugarcane treatment and the experiments. K.Y.P. detected the level of sugarcane mosaic virus (SCMV) accumulation. W.Y. assisted sugarcane materials. R.X. contributed technical software support. Y.Y. and C.L.H. wrote the manuscript with contributions from M.Q.Z.

Y. Yuan and C. Huang contributed equally to this article.

Data availability: The original contributions presented in the study are publicly available. The raw data are available at https://submit.ncbi.nlm.nih.gov/subs/sra/SUB14082371.

Funding: This research was financially supported by the China Agricultural Research System of MOF and MARA (CARS170109) and the Guangxi Key Project of the Scientific and Technological Department (Guike AA22117001).

***e*-Xtra:** Supplementary material is available online.

The author(s) declare no conflict of interest.

enhancing their pathogenic ability (Hu et al. 2018; Mengistu and Tenkegna 2021).

miRNA is a single-stranded, noncoding sRNA molecule. It comprises approximately 21 to 23 nucleotides (nt) produced through the cleavage of endogenous transcripts containing a stem-loop structure by a Dicer-like (DCL) enzyme. The mechanism of plant miRNA is complex, involving various RNA polymerase enzymes and nucleases, as well as numerous stages from transportation to processing. Gene-encoding miRNA in the nucleus is transcribed by RNA polymerase II to form a primary transcript miRNA (pri-miRNA). Then, the pri-miRNA is processed into a stem loop-structured precursor miRNA (pre-miRNA) by endonuclease DCL cleavage and released into small double-stranded RNAs (dsRNAs). The miRNA duplex is further cleaved to mature miRNA in the cytoplasm by interaction with DCL, initiating the formation of the RISC. RISCs are guided to degrade target mRNA with the argonaute protein (AGO) through complementary pairing (Akbar et al. 2022; Yekta et al. 2004). During the RNA-silencing antiviral process, in addition to miRNAs generated from endogenous plant RNA, the host processes viral RNA into small interfering RNAs (siRNAs), known as virus-derived siRNA (Ding and Voinnet 2007; Liu et al. 2021). Antiviral silencing mediated by viral siRNA plays a vital role in plant resistance to virus infection. These siRNAs can associate with host proteins to form the RISC, which directly targets and cleaves viral genomic RNA that is complementary to the siRNAs, thereby silencing the target viral genes (Ding 2010; Zhao et al. 2021).

miRNAs mediate the response of plant-pathogen interaction. The miRNA expression rapidly responds in the host plant after pathogen infection, causing changes in downstream target gene expression, thereby regulating the disease resistance of the plant host. At present, many miRNAs have been identified in plants. They can be used as an essential transcriptional regulation factor to regulate the immune response triggered by pathogen-associated molecular patterns and effectors. For example, deep miRNA sequencing of rice blast-sensitive and -resistant lines has identified some miRNAs with expression patterns related to disease resistance genes, and overexpression of miR160a and miR398b showed enhanced resistance in rice (Li et al. 2014). miR393 regulates lectin receptor-like kinases associated with lipopolysaccharide (LPS) perception in *Arabidopsis thaliana* and enhances basal resistance (Djami-Tchatchou and Dubery 2019). However, miRNAs also play a negative regulatory role in plant disease resistance. In tomatoes, miR482 and miR5300 were identified to suppress the nucleotide-binding site and leucine-rich repeat (NB-LRR) domain protein that confers resistance to *Fusarium oxysporum* (Ouyang et al. 2014). Furthermore, miR398b negatively regulates cotton immune responses to *Verticillium dahliae* via multiple targets involved in reactive oxygen species (ROS) regulation and homeostasis (Miao et al. 2022). A mechanism has been revealed in rice to enhance antiviral defense by inhibiting miRNA528 that binds to L-ascorbic acid oxidase (AO) mRNA in *ago18* null mutants, resulting in a decreased accumulation of ROS and negative regulation of rice virus resistance (Wu et al. 2017).

Our study focused on 'Fuoguo1' (FG1) derived from susceptible 'Badila', which maintains high resistance to sugarcane mosaic disease. To investigate the role of miRNA during the SCMV infection process, we performed sRNA and degradome sequencing on SCMV-infected leaves from two contrasting cultivars (SCMV-resistant FG1 and susceptible Badila) at five time points (0, 6, 18, 48, and 192 h), postinfection. The expression profile of miRNA was deciphered in response to SCMV infection with a comparative analysis between the resistant and susceptible sugarcane genotypes. Our study revealed that miRNA might affect SCMV virus replication by regulating targeted genes related to stimulus response. This study provides new insights into the role of miRNA in plant-virus interaction.

Results

Global sRNA profiling under SCMV infection

FG1 was a registered sugarcane variety resistant to SCMV. The accumulation level of SCMV RNA exhibited significant differences in virus replication dynamics between resistant and susceptible sugarcane at different time points following infection. FG1 remained at a lower level, whereas the susceptible sugarcane Badila showed exponential amplification of SCMV, especially at 18 h postinfection (Fig. 1A). To explore the role of sugarcane sRNAs in the infection of SCMV, we investigated the dynamic changes of sRNA in resistant and susceptible sugarcane. Thirty libraries generated 646,799,799 raw reads by sRNA sequencing. After quality control through removing low-quality reads and adapters, 41,046,287 clean reads were obtained. The sRNA reads contaminated with chloroplast genome (cpGenome) and ribosomal RNA (rRNA) sequences were filtered out through sequence alignment, as shown in Supplementary Table S1. The results showed that approximately 20% of the sequenced reads originated from the cpGenome, and 10% were aligned to rRNA. After filtering nonnuclear sRNAs, clean data were mapped to the FG1 genome with a high alignment rate (an average of 91%) (Supplementary Table S1). The length distribution of sRNA revealed that most reads are concentrated in the range of 21 to 24 nt (Fig. 1B). Among these, the highest number of reads corresponded to a 24-nt length, mainly phasiRNAs (phased, secondary, minor interfering RNAs), followed by miRNAs with a 21-nt length. Overall, Badila exhibited more sRNA reads than FG1, with more reads in the length range of miRNAs (21 to 22 nt) in Badila than in FG1 (Fig. 1B), indicating a higher expression abundance of miRNAs in susceptible lines.

During the assembly process, sRNA reads of 21 to 22 nt were selected for miRNA prediction. All information on genome annotation was placed in the miRNA of the file (Supplementary Table S2). The result showed that 3,158 miRNA genes were identified (618 unique sequence miRNAs), of which 1,579 were expressed as mature. The identified miRNA repertoire consisted of 660 known miRNAs, 380 novel miRNAs, and 538 potential miRNAs (Fig. 1C). The correlation-coefficient matrix plot showed that the sample from Badila at 18 h postinfection exhibited a lower correlation with the other samples, indicating that its miRNA expression might possess a distinctive characteristic (Fig. 1D). Principal component analysis (PCA) demonstrated that two samples, Badila at 6 and 18 h postinfection, maintained significant divergence when compared to the other samples. This finding suggested a more significant variation in miRNA expression levels during these two periods (Fig. 1E).

SCMV-derived siRNA and SCMV replication dynamics

To demonstrate the expression profile of siRNAs in sugarcane, we used the SCMV genome as a reference and performed filtered alignment to obtain siRNA reads. The expression trends of siRNA count in each sample were shown in Figure 2A. Notably, siRNA counts were relatively low in FG1 but significantly higher in Badila, especially at 18 h postinfection. The expression profile of SCMV-derived siRNA displayed the SCMV replication dynamics. To further understand the siRNA sequences, a distribution plot of all reads from the Badila on the SCMV genome was generated (Fig. 2B). The results revealed two enriched clusters located on the *P3* and *CP* gene sequences that were possibly related to the expression abundance of these genes.

Dominant expression of miRNA in susceptible Badila

To explore the differences in miRNA expression between SCMV-resistant and -susceptible sugarcane, we performed differential expression analysis of miRNAs in FG1 and Badila at different time points. The results revealed 566 differentially expressed miRNAs across five points (Supplementary Table S3). Venn diagram analysis showed that unique differential miRNAs dominated at 18 and 192 h postinfection (Fig. 3A). Additionally, we identified seven miRNAs that displayed differential expression across all time points, namely miRN18b, miRN18d, miRN54b, miRN54a, miRN18a, miRN18c, and miRN54d. Interestingly, the upregulated differentially expressed miRNAs in Badila were consistently more abundant than in FG1 at each time point, especially at 18 h, when viral replication peaked. The differential expression of these miRNAs in Badila was five times higher than FG1 (Fig. 3B). Furthermore, the expression heatmap was evident that miRNAs in the Badila 18 h postinfection sample exhibited significantly higher expression levels (Fig. 3C). Using the sRNAminer software, we predicted nearly 59,705 candidate target genes (including alleles) for all

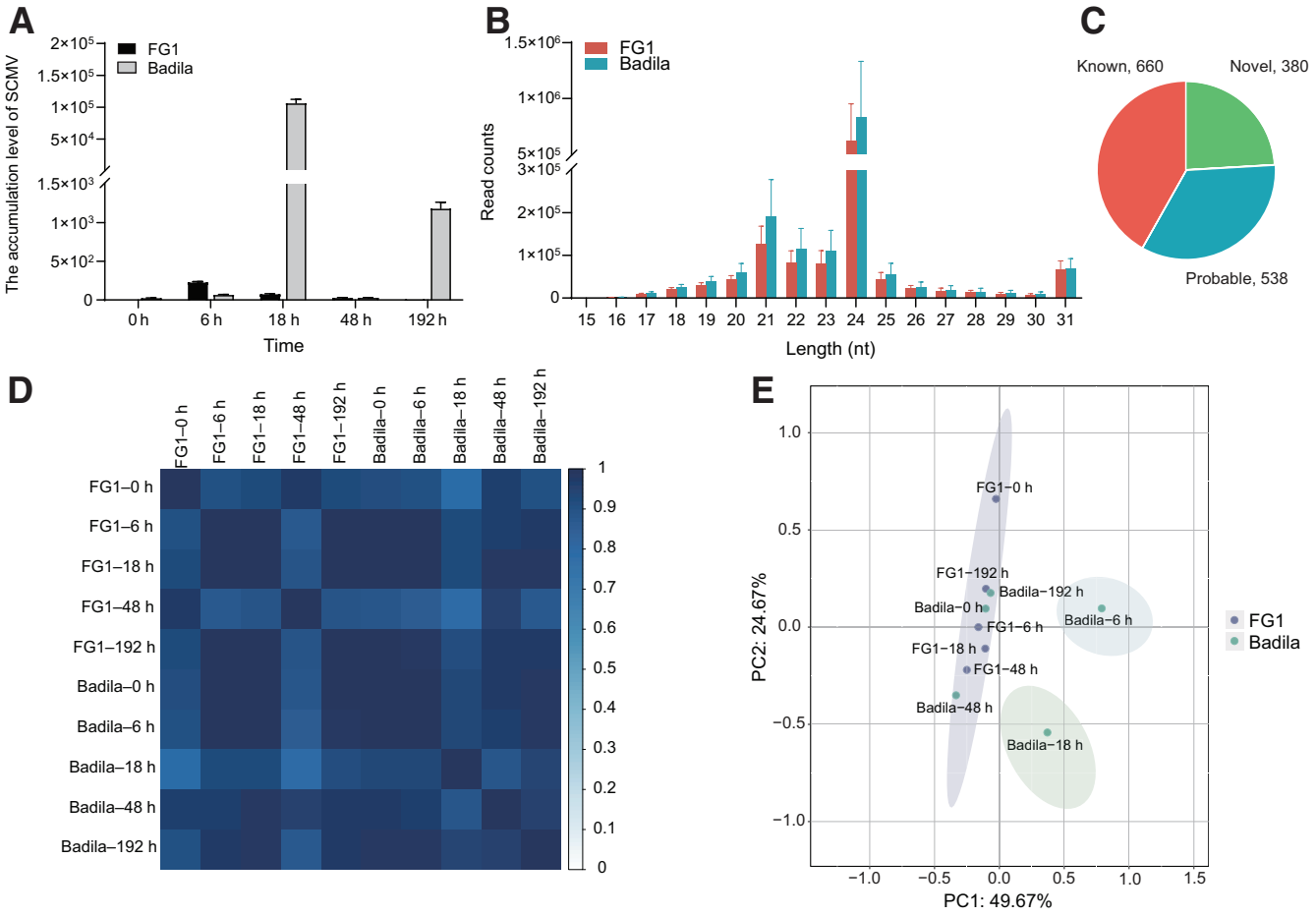

Fig. 1. Characterization of small RNAs (sRNAs) in sugarcane. **A,** The accumulation level of sugarcane mosaic virus (SCMV) RNA for SCMV-resistant 'Fuoguo1' (FG1) and -susceptible 'Badila' after infection. **B,** Length distribution of the sRNAs from the 30 libraries of SCMV-resistant FG1 and susceptible Badila. **C,** Types of identified microRNA (miRNA). **D,** Heatmap of correlation matrix. **E,** Principal component analysis (PCA).

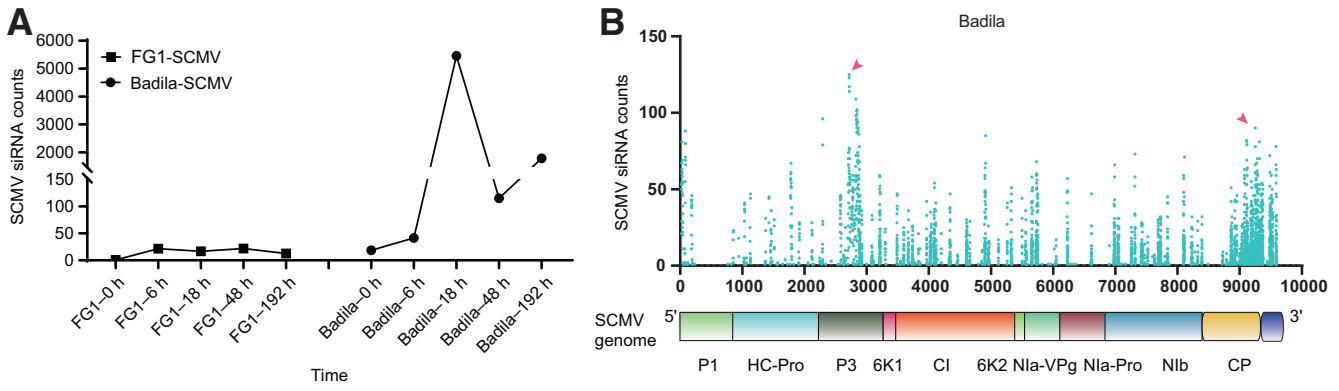

Fig. 2. Map of sugarcane mosaic virus (SCMV)-derived small interfering RNA (siRNA). **A,** SCMV-derived siRNA displays the dynamics of SCMV on two sugarcane lines; **B,** the distribution of siRNA within 'Badila' on the SCMV genome.

the differentially expressed miRNAs (Supplementary Table S4). Gene ontology (GO) enrichment analysis revealed that these genes were predominantly involved in cellular (GO:0009987) and metabolic processes (GO:0019748) and associated with molecular functions such as nucleic acid binding (GO:0005488) and catalytic activity (GO:0003824). Moreover, numerous genes were involved in biological regulation and stimulus-response processes.

miRNA exhibits a unique expression pattern associated with SCMV replication-dominant miRNA expression in susceptible Badila

miRNA is an essential component of the transcriptional regulatory network. The expression of miRNA is dynamically regulated, which means that the expression levels of miRNA can vary at different time points or under different environmental conditions. The k-means clustering was performed to investigate the temporal dynamic of miRNA for resistant and susceptible sugarcane after SCMV infection. The miRNA expression patterns were categorized into four clusters, with cluster 1 encompassing the largest number of miRNAs and exhibiting the most significant differential expression change (Fig. 4A; Supplementary Table S5). Cluster 1, containing 388 miRNAs, shared a typical expression pattern in which genes maintained low expression levels throughout various time points in FG1 but showed a rapid transcriptional upregulation at 18 h postinfection in the susceptible Badila. Remarkably, this expression pattern displayed a significant positive correlation with the replication profile of SCMV in both samples. Among cluster 1, miRNAs were highly expressed 18 h postinfection for Badila, with the most significant differences including the miR171 and miR160 families (Supplementary Fig. S1; Supplementary Table S6). The miRN54a was overexpressed explicitly in Badila and not expressed in FG1.

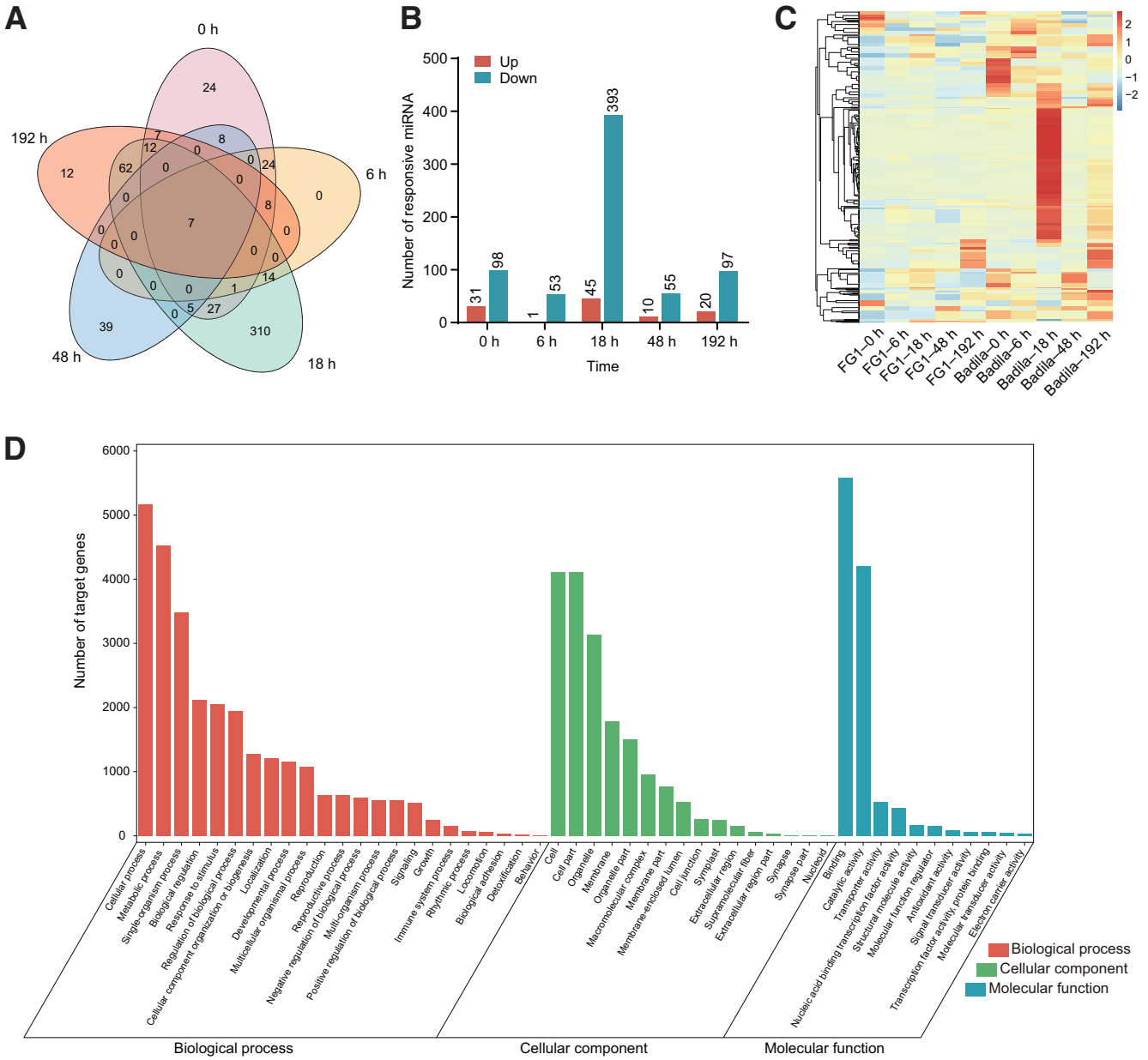

Fig. 3. Differential expression analysis of microRNA (miRNA). **A,** Venn diagram of differential miRNA between 'Fuoguo1' (FG1) and 'Badila' at each stage. **B,** The up- or downregulated miRNA by FG1 compared with Badila. **C,** Heatmap of differentially expressed miRNA. **D,** Gene ontology (GO) enrichment analysis of target genes predicted by miRNA.

Identification of miRNA target genes through degradome sequencing

We identified a dominant miRNA cluster whose expression trend is associated with viral replication, suggesting the possibility of their crucial role in facilitating viral replication in the host. Based on differently expressed miRNA sequences, over 16,076 candidate target genes were identified using degradation group prediction (category < 3). At the critical time point of 18 h postinfection, the number of target genes regulated by cluster 1 miRNAs exhibited a significant difference, in which 931 target genes were identified in FG1, while 2,305 target genes were identified in Badila (Supplementary Table S7). The count in Badila is approximately 2.5 times higher than in FG1 (Fig. 4A), indicating more mRNA-silencing events in Badila at 18 h postinfection, which is characterized by a higher abundance of miRNA target genes. Comparing the overlap of target genes between FG1 and Badila at the critical period (18 h), the Venn diagram showed that 449 genes were shared, but a more significant proportion of target genes were exclusive to Badila (Fig. 4B). We further explored the functional implications of these differentially regulated target genes. GO enrichment analysis revealed a significantly higher number of genes in Badila compared to FG1, displaying a notable enrichment in the biological process associated with stimulus response (GO:0050896) and cellular components related to the plastid (GO:0009536) (Fig. 4C).

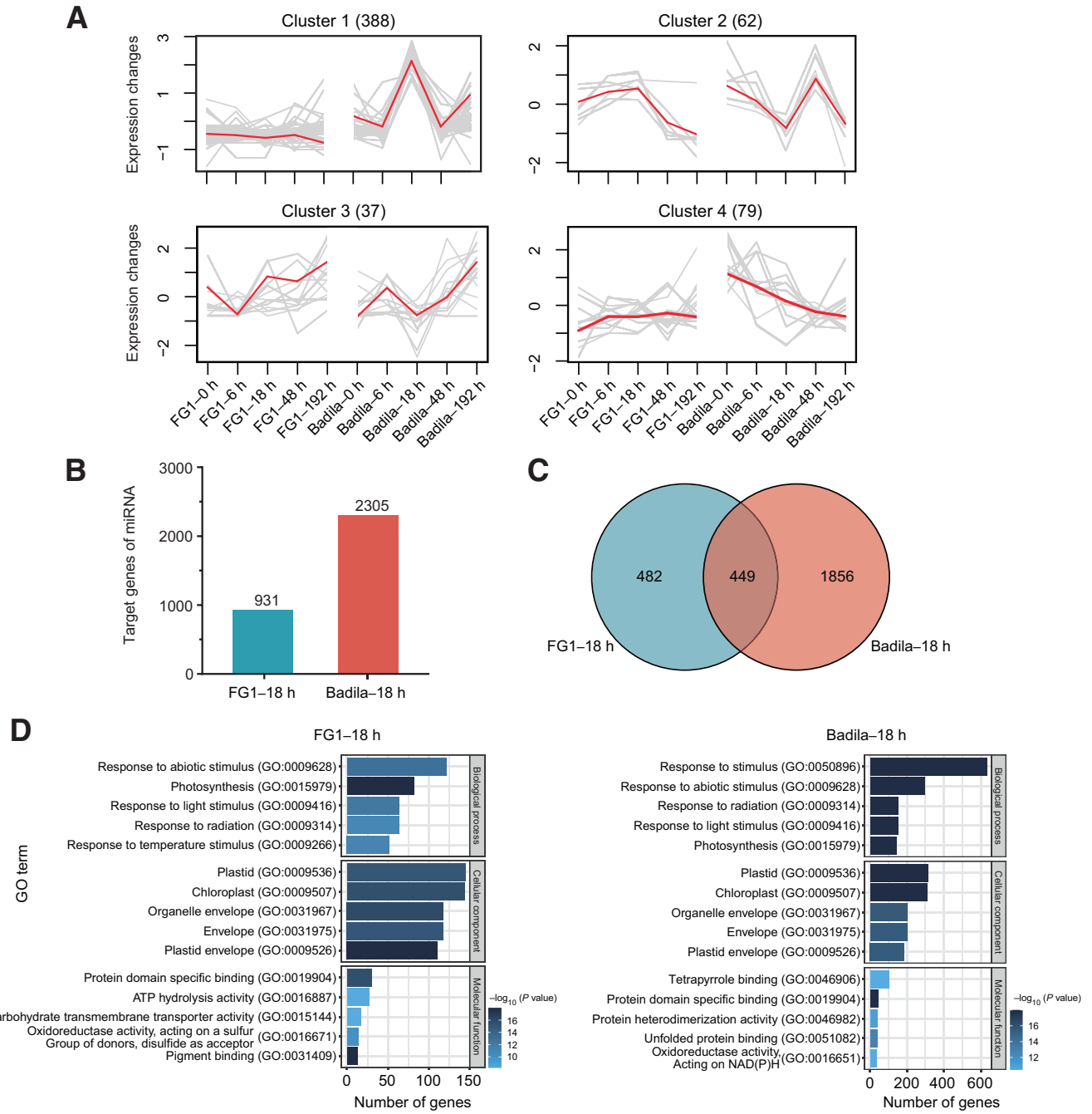

Fig. 4. Clustering of microRNA (miRNA) expression trends and functional analysis of target genes. **A,** k-means clustering showing the miRNA expression profiles. **B,** The number of differential miRNA target genes based on degradome 18 h after infection. **C,** Venn diagram of target genes. **D,** Gene ontology (GO) enrichment analysis of miRNA target genes.

Our findings indicated that miRNAs were predominantly upregulated in the susceptible Badila, while miRNA expression in FG1 remained stable at different time points after SCMV treatment; miRNAs displayed significantly in response to SCMV infection. The expression pattern of miRNA was consistent with the viral replication curve, suggesting a close association between miRNA and viral replication. Identified miRNA and their target genes predominantly function in stimulus response and might be involved in the SCMV replication dynamic in susceptible Badila.

Constructing miRNA-genes regulatory network

miRNA actively responding to SCMV replication in susceptible Badila showed that their target genes were significantly enriched in a biological process-related stimulus response. A total of 633 target genes are involved in stimulus response and corresponding different expression miRNA. The functional annotation showed that most of these genes regulated biological processes (Supplementary Table S8). Domain analysis showed that the top families included protein kinase, small heat shock protein Hsp20, calmodulin, bZIP, and MYB transcription factor families (Supplementary Fig. S2). A multi-omics integrative analysis combined with sRNA sequencing and degradation sequencing was performed. Firstly, we obtained these target protein interaction networks (PPI) using the STRING database (https://string-db.org/). Next, regulatory relationships were determined between miRNAs and corresponding target genes based on degradome. We reconstructed the regulatory network with the fold difference of miRNA expression at 18 h. We displayed the miRNA-gene interaction network using the Cytoscape software (Fig. 5). This network showed 33 different expression miRNAs targeting 160 genes involved in stimulus response, including several core miRNAs. miR5079 with maximum node degree regulated the most target genes. The most considerable fold change was found in miR160, showing the most significant expression difference at 18 h postinfection. We identified some high-frequency node target genes involved in stimulus response, such as encoding chaperone protein CLPB1, heat shock protein HSP81-1, and calcium-binding proteins CML32 and CML24. Meanwhile, some target genes were involved in defense response, including transcription factors TGAL6 and NAC048, E3 ubiquitin-proteins NPR2 and NPR3, and cinnamoyl-CoA

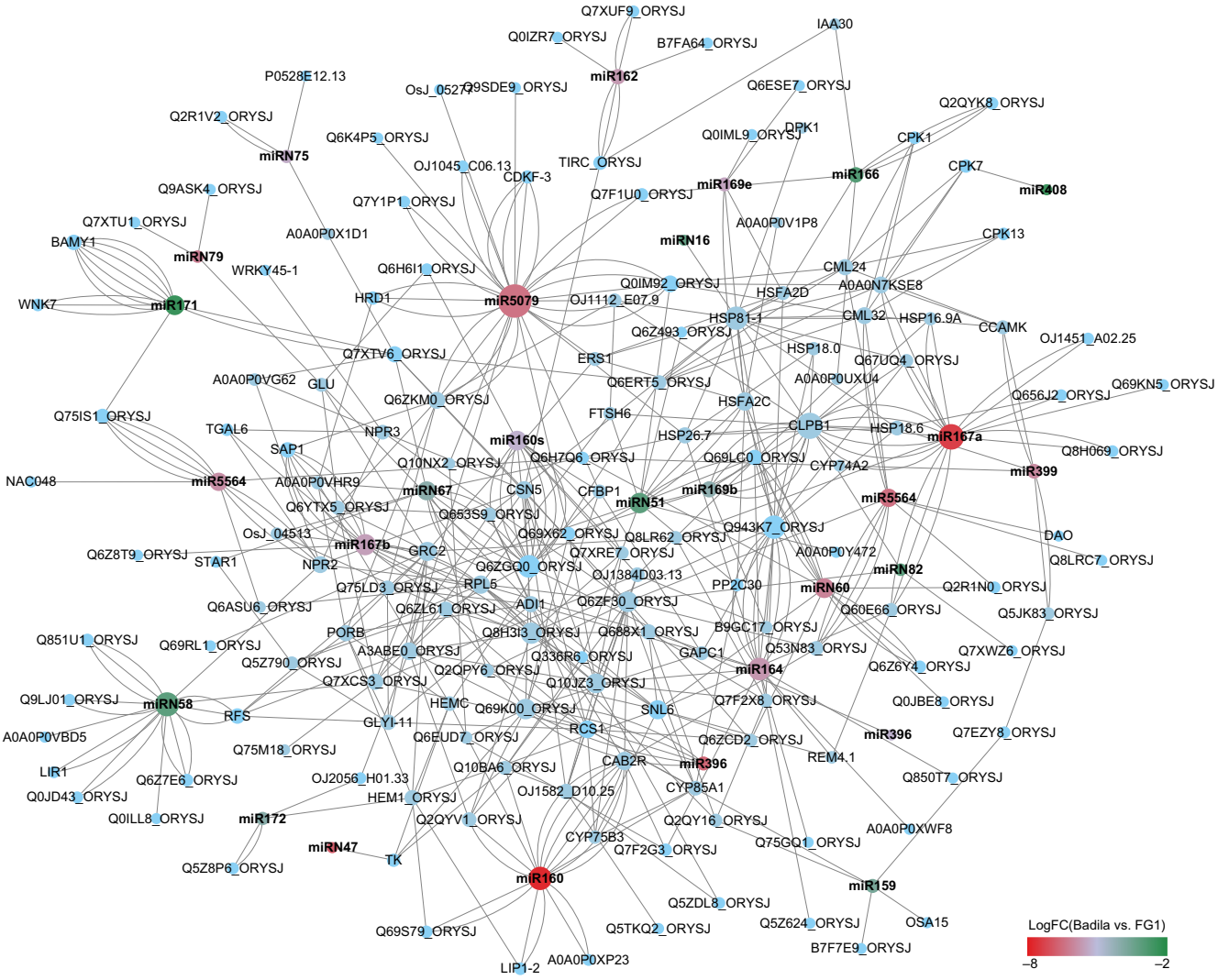

Fig. 5. Regulatory networks of microRNA (miRNA)–messenger RNA (mRNA) in response to sugarcane mosaic virus (SCMV). The gradient-colored circles represent the fold change (FC) of miRNA expression. The blue circles represent the target genes related to stress response based on the degradation group. The size of the circles represents the number of nodes. The protein interaction networks (PPI) interaction between target genes provided a framework for constructing regulatory networks. Multiple lines between two genes were due to the characteristics of multiple alleles in sugarcane.

reductase-like SNL6. These genes were negatively regulated by highly expressed miRNAs in Badila, which might be the reason for attenuated defense against SCMV infection.

Verification of differential miRNAs and target genes

We further validated the highest expression differences with miRNA160. Seventy miR160 families were identified, including two differentially expressed miRNA subtypes in sugarcane. The first subtype expressed the same miRNA sequence "GCGTGCGAGGTGCCAAGCATGG", consisting of miR160d-Known-3p-star, miR160e-Known-3p-star, miR160f-Known-3p-star, miR160g-Known-3p-star, miR160h-Known-3p-star, and miR160i-Known-3p-star. miR160d was considered the representative miRNA of this subtype. The second subtype expressing an miRNA sequence, "GCGT GCAAGGAGCCAAGCATG", included miR160ad-Probable-5p-mature, miR160ae-Known-3p-star, miR160af-Known-3p-star, miR160ag-Known-3p-star, miR160ah-Known-3p-star, and miR160ai-Known-3p-star. miR160a was considered the representative miRNA of the second subtype. The expression of these miRNAs was verified through the alignment of sRNA sequencing data using IGV-sRNA software (https://gitee.com/CJchen/IGV-sRNA). The validation results showed significant differences in read count for miR160d, miR160e, and miR160h of the first subtype. In contrast, only miR160ae of the second subtype exhibited differential expression in response to resistance or susceptibility to SCMV (Fig. 6A).

Furthermore, quantitative real-time PCR (qRT-PCR) was used to validate the differential miRNA expression. The qRT-PCR results showed consistent relative expression levels and expression trends for three miRNA sequences. Both miR160d and miR160ae were found to have significantly higher expression levels in Badila at 18 h postinfection (Fig. 6B). Additionally, a target gene with a repetitive leucine-rich sequence, encoded by the LRR gene (SoZg.04B006970.1), was identified among the degradation targets of miR160d/e/h. The qRT-PCR depicted the expression trend of LRR, suggesting the negative expression correlation between LRR and miR160d (Fig. 6C).

Discussion

Plants inevitably encounter various biotic stresses throughout their growth, prompting the development of adaptive mechanisms during their long-term evolution. miRNAs are pivotal in regulating plant development and responses to environmental stresses, including interaction with viruses (Mengistu and Tenkegna 2021; Raza et al. 2023). Sugarcane, a globally significant crop for sugar production and a promising green carbon source in biomass (Karp et al. 2022), needs a comprehensive understanding of miRNA-mediated regulatory mechanisms in response to viral infections. Hence, investigating how resistant sugarcane variety FG1 and susceptible Badila respond to SCMV becomes crucial for understanding the detailed regulatory network involved. This research enhances our understanding of miRNA-generated responses in sugarcane and contributes to the strategies for enhancing resistance against SCMV infections.

sRNA molecules, particularly miRNAs, play an essential role in plant defense against viral infections (Lu et al. 2008; Mengistu and Tenkegna 2021). Specific miRNAs target viral genomes or plant host genes associated with viral infections, thereby regulating the antiviral response of plants and enhancing immune capabilities (Kong et al. 2022). Notably, recent studies have revealed that viruses possess mechanisms to evade the host plant immune response during plant-virus interaction by modulating the expression of plant miRNAs. Plant miRNAs could counteract viral infections through negative regulation (Wu et al. 2015) and are profoundly involved in this defense mechanism against viral invasions.

Upon invading a host, the virus spreads and replicates throughout the plant to induce disease. During this stage, a dynamic interaction occurs between the virus and host, with the virus striving to establish infection while the host endeavors to resist it. Our research findings showed that resistant sugarcane FG1 retained a low viral load. Contradictorily, the replication curve of the SCMV infection on the Badila leaves showed inadequate resistance to SCMV during the confrontation of the virus and host cells. The observed transition trend of virus replication from exponential expansion to stabilization was likely caused by the movement of SCMV in the Badila leaves after infection.

In this study, we investigated the expression differences of miRNAs in resistant sugarcane FG1 and susceptible Badila at different time points postinfection by sRNA sequencing and degradome sequencing techniques. Notably, a higher number of sRNA reads were generated in Badila after infection as compared to FG1, and the assembled miRNA reads also showed a similar abundance advantage. The analysis highlighted the primary contributions derived from the rapid expansion of miRNA in Badila following SCMV infection. Additionally, the expression profile of miRNAs postinfection revealed characteristic differences in the Badila at 18 h postinfection, as elucidated through differential expression and sample correlation analysis.

Combined with the absolute quantification and transcriptional expression analysis of SCMV, as mentioned earlier, the 18-h postinfection timepoint was identified as the viral replication phase. During this phase, there was notable and abrupt enhancement of miRNA expression. Similar phenomena have been reported in the response of rice-to-rice stripe virus (RSV) infection, where the expression level of miR160, miR166, miR167, miR171, and miR396 families increased (Du et al. 2011). Our research specifically identified a significant responsiveness of miR160 to SCMV. The miR160 family is involved in diverse functions, initially identified in *Arabidopsis* as regulators of auxin-response factors (Rhoades et al. 2002). The downregulation of OsmiR160 targeting OsARF18 resulted in growth and development defects in rice and caused auxin signaling (Huang et al. 2016). Ectopic expression of miR160 induced super-sensitivity to auxin in soybeans, among other effects (Turner et al. 2013). Furthermore, miR160 played a crucial regulatory role in biotic stress, demonstrating positive feedback during the response to cassava anthracnose disease (Pinweha et al. 2015). Previous research showed that miR160 played a crucial role in plant defense against viruses and insects such as cucumber mosaic virus and RSV (Bazzini et al. 2007; Du et al. 2011; Kundu et al. 2017). This regulatory role is possibly exerted through the induction of RNA-silencing pathway components.

Among the target genes of miR160, seven genes encoding the CAB2R protein (including alleles or homologous genes) are located at the chloroplast thylakoid membrane, which is associated with the light-harvesting complex (LHC), and function as light receptors tightly linked to chloroplast development. Besides their role as the site of photosynthesis, chloroplasts are crucial components of plant defense responses and actively participate in plant-virus interactions. Notably, chloroplasts are the primary target for successfully infecting plant viruses into hosts. High expression of miR160 exacerbated the inhibitory regulation of the CABR2 gene, possibly resulting in a weakening of chloroplast defense. Furthermore, we also identified the candidate target gene LRR of miR160, which exhibits a negative regulatory expression pattern with miR160. However, this gene has been relatively understudied regarding its function, and regulatory mechanisms require further investigation.

Based on integrative analysis using multi-omics data, we constructed an miRNA-mRNA regulatory network involving stress response and displayed several core miRNAs. The noteworthy findings on miR5079 involved in heat stress tolerance have been reported (Mangrauthia et al. 2017). Our research unveils novel facts about miR5079, elucidating its potential functions related to virus response. miR167 has been recognized as a significant contributor to resistance against maize chlorotic mottle virus (MCMV) through the Zma-miR167-ARF3/30-PAO1 signaling pathway (Liu et al. 2022). Intriguingly, our research diverges from previous investigations, as we observed the induction of miR167 by SCMV. Contrary to its role in MCMV resistance in maize, miR167 did not exhibit such a response to SCMV, suggesting that the functions of miR167 might vary in response to distinct viruses or hosts.

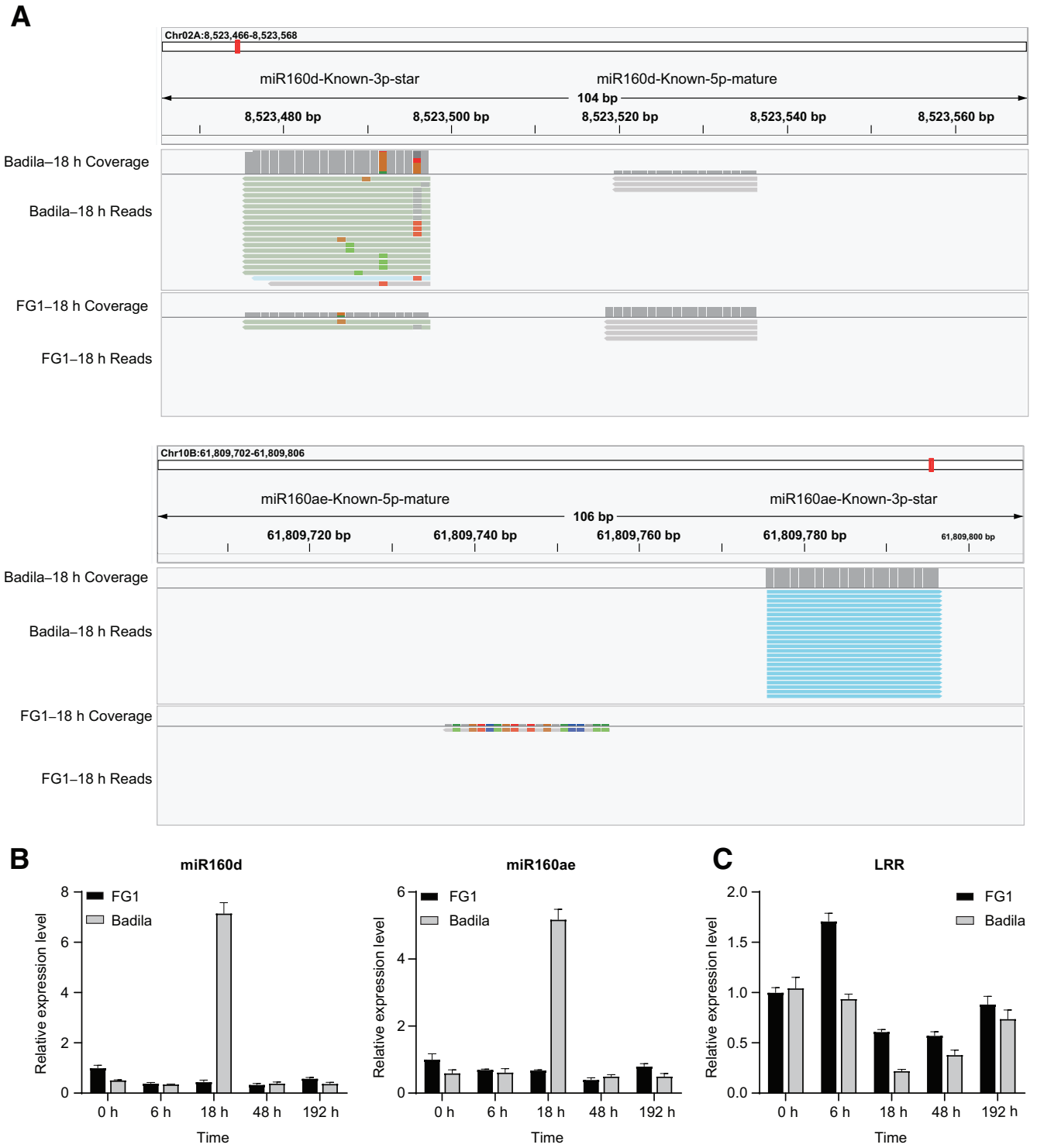

Fig. 6. The significant differential expression of miR160 between resistant and susceptible sugarcane. **A,** Genome browser showing the alignment of miR160 reads at 18 h after infection. **B and C,** Results of quantitative real-time PCR (qRT-PCR) showing the accumulation profile of miR160 and targets among the time points after infection. Relative expression level (REL) was calculated using 'Fuoguo1' (FG1) without treatment (FG1–0 h) as a control. LRR, leucine-rich repeat.

Further investigations are required to better understand specific functions associated with identified target genes. Some target genes were identified within this regulatory network as involved in plant defense. NPR2 and NPR3, belonging to the BTB/POZ domain and ankyrin repeat-containing protein, are reportedly involved in the defense response against bacterial blight disease in rice (Yuan et al. 2007). The transcription factors involved in defense response, such as TGAL6 (Fitzgerald et al. 2005) and NAC048 (Nakashima et al. 2007), were found to be negatively regulated by differentially expressed miRNAs.

In summary, many miRNAs were positively expressed with SCMV replication, forming a distinct cluster. The functions of the miRNA-clustered target genes, through degradome sequencing data, are significantly enriched in stimulus response, suggesting a regulatory mechanism where SCMV induces the expression of miRNAs, which negatively regulate stress response genes involved in defense mechanisms. This regulatory process might attenuate SCMV resistance, enabling the virus to colonize the host successfully. These findings highlight the involvement of miRNAs in the regulatory mechanism of SCMV virus infection and provide a molecular foundation for understanding host defense against viral infections.

Materials and Methods

Plant materials and treatment

Sugarcane (*S. officinarum*) resistant genotype FG1 is registered in the Ministry of Agriculture and Rural Affairs of China Trial Registry (registration number: GPD Sugarcane [2022] 450016), sustaining high resistance against SCMV infection and was obtained by somatic mutation of susceptible cultivar Badila (Nanning, Guangxi, China). Stable growth conditions were supplied at 24 to 28°C with a 16/8-h light/dark photoperiod. The first leaf, being 1 month old (at the four- to five-leaf stage) and grown above the ligule, was mechanically infected with sap (at 6:00 pm). Sap was prepared using crude extract of SCMV-infected leaves with phosphate buffer (PB) and was stained using 80-mesh quartz. Inoculation was performed using fingers which lightly reciprocate friction five times. Leaves were wrapped with fresh film to maintain humidity. After infection, sampling was collected at different time points (0, 6, 18, 48, and 192 h). Each leaf was cut 15 cm, which distributed three inoculation sites, with each being about 1-cm wide. A total of 30 samples from five points were collected, with each being from Badila and FG1. Two replicates from each sample were collected for further analysis. A total of 30 sRNA and 10 degradome libraries were constructed. Three sRNA library samples (biological replicates) from the same time point were merged into one degradome library.

sRNA and degradome library construction

To construct an sRNA library, total RNA was extracted using TRIzol reagent (Invitrogen, Carlsbad, CA, U.S.A.) according to the manufacturer's guidelines. The RNA concentration and purity were quantified using NanoDrop ND-1000 (NanoDrop, Wilmington, DE, U.S.A.). The integrity of RNA was evaluated by Bioanalyzer 2100 (Agilent, CA, U.S.A.) and verified by agarose gel electrophoresis. The experimental procedure followed the standard steps provided by the Illumina company, including library preparation and sequencing experiments. An sRNA sequencing library was obtained using TruSeq Small RNA Sample Prep Kits (Illumina, San Diego, U.S.A.). The constructed library was sequenced using Illumina Hiseq2500 with a single-end reading length of 1×50 bp.

To construct a degradome complementary DNA (cDNA) library, poly-A RNA was purified from plant total RNA (20 μg) using poly-T oligo-attached magnetic beads in two rounds of purification for each sample. The RNA ligase ligated the adapters to the 5′ end of the 3′ cleavaged mRNA. Reverse transcription was performed to synthesize the first strand of cDNA with a 3′-adapter random primer. Following the vendor's recommended protocol, the 50-bp single-end sequencing was performed on an Illumina HiSeq 2500 (LC Bio, China).

We have constructed 30 sRNA libraries and a degradome cDNA library, respectively. Constructions of libraries and RNA sequencing were performed by the Hangzhou Lianchuan Biotechnology Co., Ltd (Hangzhou, Zhejiang, China).

miRNA prediction and quantification

The raw sequencing data was assembled and analyzed using sRNAminer software (https://github.com/kli28/sRNAminer). The FG1 genome was used as the reference genome (Muqing Zhang and Jisen Zhang; *unpublished data*). The currently known miRNA was downloaded from the database miRBase (https://mirbase.org/). The sRNA quality was controlled by filtering related databases from NCBI, including all rRNA and cpGenome databases. The sRNAseqAdapterPrediction program was used to predict the adapter for clean_data. The sRNA sequencing data adapter was removed by sRNAseqAdapterRemover and deduplicated by sRNAseqCollasper. rRNA and cpGenome databases were mapped to filter contamination of rRNA and organelle genome reads. Filtering reads were mapped to the FG1 genome by sRNAseqAlignmentFormater. Based on the miRBase database, the identification of miRNA used miRNAminerCLI (--matureColIndex 6 --starColIndex 7 --starAbundanceIndex 11). sRNAQuantify quantified the abundance of miRNA expression, and standardized expression information (RPTM) was obtained. The prediction of sRNA produced by SCMV was the same as above, except that the SCMV genome (NC_003398.1) was used as the reference genome.

miRNA expression analysis

Sample correlation coefficient analysis and PCA were performed by R package corrplot (Wei and Simko 2021) and vegan (Dixon 2003). Differential expression analysis of miRNA was conducted between FG1 and Badila at the same time points by DESeq2 (Love et al. 2014) and identified differential miRNA (fold change > 1, P value < 0.05). Venn diagrams were drawn by Tbtools (Chen et al. 2020), displaying the similarities and differences of differentially expressed genes at different time points. All heatmaps were generated with the R package heatmap (Zhang et al. 2016). sRNAminer (TargetSoPipe) was used to predict candidate target genes of miRNAs based on FG1 genome data. The expression trend cluster for differential miRNA was analyzed using the R package Mfuzz (Kumar and Futschik 2007). The GO annotation for each gene comes from the FG1 genome functional annotation. GO enrichment evaluation was performed using TBtools and followed by visualization using the R package ggplot2 (Ginestet 2011). All GO categories with P values $<$ 0.00001 were considered enrichment options.

Identification of miRNA target genes using degradome sequencing

Degradome sequencing raw data was executed for quality control by removing the adapter from sRNAminer (sRNAseqAdapterPrediction and sRNAseqAdapterRemover) packages. Target genes of differential miRNA analysis were identified in degradome sequencing data using CleaveLand4 (v4.5, https://github.com/MikeAxtell/CleaveLand4/archive/refs/heads/master.zip (Addo-Quaye et al. 2009) with default parameters. Detailed information about each target gene corresponding to an miRNA was generated (Supplementary Table S9). The CleaveLand4 software only predicted one miRNA at a time. The first used type 1 model parameters that align gradient data sRNA queries

and analyze (-e -u -n). Then, the degradation group file remained freezing, and different miRNA sequences were performed to identify the type 2 model (-d -u -n).

qRT-RCR analysis

We assessed the relative expression level of the *CP* gene to indicate the accumulation level of SCMV RNA using qRT-PCR. The tailing-based method was used to quantify miRNA. RNA samples were reverse transcribed to obtain cDNA with poly-A using an miRNA one-step cDNA synthesis kit (Takara 638315) following the kit's protocol. The qRT-PCR with three biological replications was performed with SYBR green on the Roche Lightcyler 480 instrument using the SYBR fluorescence quantification method (Takara, RR820A). The *U6* gene was selected as the miRNA reference gene. The forward primers were designed on the miRNA sequence, and a few nucleotides were added at the 5′ end according to the specific requirements. The reagent kit provides reverse primers of miRNA, but the sequence was unpublished due to being intellectual property. mRNA quantification referenced the previous qRT-RCR protocol (Yuan et al. 2021). The primer sequences are shown in Supplementary Table S10.

Literature Cited

Addo-Quaye, C., Miller, W., and Axtell, M. J. 2009. CleaveLand: A pipeline for using degradome data to find cleaved small RNA targets. Bioinformatics 25:130-131.

Akbar, S., Wei, Y., and Zhang, M.-Q. 2022. RNA interference: Promising approach to combat plant viruses. Int. J. Mol. Sci. 23:5312.

Baulcombe, D. 2004. RNA silencing in plants. Nature 431:356-363.

Bazzini, A. A., Hopp, H. E., Beachy, R. N., and Asurmendi, S. 2007. Infection and coaccumulation of tobacco mosaic virus proteins alter microRNA levels, correlating with symptoms and plant development. Proc. Natl. Acad. Sci. U.S.A. 104:12157-12162.

Chen, C., Chen, H., Zhang, Y., Thomas, H. R., Frank, M. H., He, Y., and Xia, R. 2020. TBtools: An integrative toolkit developed for interactive analyses of big biological data. Mol. Plant 13:1194-1202.

Csorba, T., Pantaleo, V., and Burgyán, J. 2009. RNA silencing: An antiviral mechanism. Adv. Virus Res. 75:35-71.

Ding, S.-W. 2010. RNA-based antiviral immunity. Nat. Rev. Immunol. 10:632-644.

Ding, S.-W., and Voinnet, O. 2007. Antiviral immunity directed by small RNAs. Cell 130:413-426.

Dixon, P. 2003. VEGAN, a package of R functions for community ecology. J. Veg. Sci. 14:927-930.

Djami-Tchatchou, A. T., and Dubery, I. A. 2019. miR393 regulation of lectin receptor-like kinases associated with LPS perception in *Arabidopsis thaliana*. Biochem. Biophys. Res. Commun. 513: 88-92.

Du, P., Wu, J., Zhang, J., Zhao, S., Zheng, H., Gao, G., Wei, L., and Li, Y. 2011. Viral infection induces expression of novel phased microRNAs from conserved cellular microRNA precursors. PLoS Pathog. 7:e1002176.

Fitzgerald, H. A., Canlas, P. E., Chern, M.-S., and Ronald, P. C. 2005. Alteration of TGA factor activity in rice results in enhanced tolerance to *Xanthomonas oryzae* pv. *oryzae*. Plant J. 43:335-347.

Gao, B., Cui, X.-W., Li, X.-D., Zhang, C.-Q., and Miao, H.-Q. 2011. Complete genomic sequence analysis of a highly virulent isolate revealed a novel strain of *Sugarcane mosaic virus*. Virus Genes 43: 390-397.

Ginestet, C. 2011. ggplot2: Elegant graphics for data analysis. J. R. Stat. Soc. Ser. A Stat. Soc. 174:245-246.

Guo, Z., Li, Y., and Ding, S.-W. 2019. Small RNA-based antimicrobial immunity. Nat. Rev. Immunol. 19:31-44.

Hu, F., Lei, R., Deng, Y.-F., Wang, J., Li, G.-F., Wang, C.-N., Li, Z.-H., and Zhu, S.-F. 2018. Discovery of novel inhibitors of RNA silencing suppressor P19 based on virtual screening. RSC Adv. 8:10532-10540.

Huang, J., Li, Z., and Zhao, D. 2016. Deregulation of the *Os*miR160 target gene *OsARF18* causes growth and developmental defects with an alteration of auxin signaling in rice. Sci. Rep. 6:29938.

Karp, S. G., Burgos, W. J. M., Vandenberghe, L. P. S., Diestra, K. V., Torres, L. A. Z., Woiciechowski, A. L., Letti, L. A. J., Pereira, G. V. M., Thomaz-Soccol, V., Rodrigues, C., de Carvalho, J. C., and Soccol, C. R. 2022. Sugarcane: A promising source of green carbon in the circular bioeconomy. Sugar Tech 24:1230-1245.

Kong, X., Yang, M., Le, B. H., He, W., and Hou, Y. 2022. The master role of siRNAs in plant immunity. Mol. Plant Pathol. 23:1565-1574.

Kumar, L., and Futschik, M. E. 2007. Mfuzz: A software package for soft clustering of microarray data. Bioinformation 2:5-7.

Kundu, A., Paul, S., Dey, A., and Pal, A. 2017. High throughput sequencing reveals modulation of microRNAs in *Vigna mungo* upon *Mungbean yellow mosaic India virus* inoculation highlighting stress regulation. Plant Sci. 257:96-105.

Lakshmanan, P., Geijskes, R. J., Aitken, K. S., Grof, C. L. P., Bonnett, G. D., and Smith, G. R. 2005. Sugarcane biotechnology: The challenges and opportunities. In Vitro Cell. Dev. Biol. Plant 41:345-363.

Li, Y., Lu, Y.-G., Shi, Y., Wu, L., Xu, Y.-J., Huang, F., Guo, X.-Y., Zhang, Y., Fan, J., Zhao, J.-Q., Zhang, H.-Y., Xu, P.-Z., Zhou, J.-M., Wu, X.-J., Wang, P.-R., and Wang, W.-M. 2014. Multiple rice microRNAs are involved in immunity against the blast fungus *Magnaporthe oryzae*. Plant Physiol. 164:1077-1092.

Liu, P., Zhang, X., Zhang, F., Xu, M., Ye, Z., Wang, K., Liu, S., Han, X., Cheng, Y., Zhong, K., Zhang, T., Li, L., Ma, Y., Chen, M., Chen, J., and Yang, J. 2021. A virus-derived siRNA activates plant immunity by interfering with ROS scavenging. Mol. Plant 14:1088-1103.

Liu, X., Liu, S., Chen, X., Prasanna, B. M., Ni, Z., Li, X., He, Y., Fan, Z., and Zhou, T. 2022. Maize *miR167-ARF3/30-polyamine oxidase 1* module-regulated H_2O_2 production confers resistance to maize chlorotic mottle virus. Plant Physiol. 189:1065-1082.

Love, M. I., Huber, W., and Anders, S. 2014. Moderated estimation of fold change and dispersion for RNA-seq data with DESeq2. Genome Biol. 15:550.

Lu, Y.-d., Gan, Q.-h., Chi, X.-y., and Qin, S. 2008. Roles of microRNA in plant defense and virus offense interaction. Plant Cell Rep. 27:1571-1579.

Mangrauthia, S. K., Bhogireddy, S., Agarwal, S., Prasanth, V. V., Voleti, S. R., Neelamraju, S., and Subrahmanyam, D. 2017. Genome-wide changes in microRNA expression during short and prolonged heat stress and recovery in contrasting rice cultivars. J. Exp. Bot. 68:2399-2412.

Mengistu, A. A., and Tenkegna, T. A. 2021. The role of miRNA in plant-virus interaction: A review. Mol. Biol. Rep. 48:2853-2861.

Miao, Y., Chen, K., Deng, J., Zhang, L., Wang, W., Kong, J., Klosterman, S. J., Zhang, X., Aierxi, A., and Zhu, L. 2022. miR398b negatively regulates cotton immune responses to *Verticillium dahliae* via multiple targets. Crop J. 10:1026-1036.

Nakashima, K., Tran, L.-S. P., Van Nguyen, D., Fujita, M., Maruyama, K., Todaka, D., Ito, Y., Hayashi, N., Shinozaki, K., and Yamaguchi-Shinozaki, K. 2007. Functional analysis of a NAC-type transcription factor OsNAC6 involved in abiotic and biotic stress-responsive gene expression in rice. Plant J. 51:617-630.

Ouyang, S., Park, G., Atamian, H. S., Han, C. S., Stajich, J. E., Kaloshian, I., and Borkovich, K. A. 2014. MicroRNAs suppress NB domain genes in tomato that confer resistance to *Fusarium oxysporum*. PLoS Pathog. 10:e1004464.

Pinweha, N., Asvarak, T., Viboonjun, U., and Narangajavana, J. 2015. Involvement of *miR160*/*miR393* and their targets in cassava responses to anthracnose disease. J. Plant Physiol. 174:26-35.

Raza, A., Charagh, S., Karikari, B., Sharif, R., Yadav, V., Mubarik, M. S., Habib, M., Zhuang, Y., Zhang, C., Chen, H., Varshney, R. K., and Zhuang, W. 2023. miRNAs for crop improvement. Plant Physiol. Biochem. 201:107857.

Rhoades, M. W., Reinhart, B. J., Lim, L. P., Burge, C. B., Bartel, B., and Bartel, D. P. 2002. Prediction of plant microRNA targets. Cell 110:513-520.

Turner, M., Nizampatnam, N. R., Baron, M., Coppin, S., Damodaran, S., Adhikari, S., Arunachalam, S. P., Yu, O., and Subramanian, S. 2013. Ectopic expression of miR160 results in auxin hypersensitivity, cytokinin hyposensitivity, and inhibition of symbiotic nodule development in soybean. Plant Physiol. 162:2042-2055.

Viswanathan, R., and Balamuralikrishnan, M. 2005. Impact of mosaic infection on growth and yield of sugarcane. Sugar Tech 7:61-65.

Wei, T.-Y., and Simko, V. 2021. corrplot: Visualization of a correlation matrix. Version 0.92. https://cran.r-project.org/package=corrplot

Wu, J., Yang, R., Yang, Z., Yao, S., Zhao, S., Wang, Y., Li, P., Song, X., Jin, L., Zhou, T., Lan, Y., Xie, L., Zhou, X., Chu, C., Qi, Y., Cao, X., and Li, Y. 2017. ROS accumulation and antiviral defence control by microRNA528 in rice. Nat. Plants 3:16203.

Wu, J., Yang, Z., Wang, Y., Zheng, L., Ye, R., Ji, Y., Zhao, S., Ji, S., Liu, R., Xu, L., Zheng, H., Zhou, Y., Zhang, X., Cao, X., Xie, L., Wu, Z., Qi, Y., and Li, Y. 2015. Viral-inducible Argonaute18 confers broad-spectrum virus resistance in rice by sequestering a host microRNA. eLife 4: e05733.

Xie, J., Jiang, T., Li, Z., Li, X., Fan, Z., and Zhou, T. 2021. Sugarcane mosaic virus remodels multiple intracellular organelles to form genomic RNA replication sites. Arch. Virol. 166:1921-1930.

Yekta, S., Shih, I.-h., and Bartel, D. P. 2004. MicroRNA-directed cleavage of *HOXB8* mRNA. Science 304:594-596.

Yuan, Y., Yang, X., Feng, M., Ding, H., Khan, M. T., Zhang, J., and Zhang, M. 2021. Genome-wide analysis of R2R3-MYB transcription factors family in the autopolyploid *Saccharum spontaneum*: An exploration of dominance expression and stress response. BMC Genomics 22: 622.

Yuan, Y., Zhong, S., Li, Q., Zhu, Z., Lou, Y., Wang, L., Wang, J., Wang, M., Li, Q., Yang, D., and He, Z. 2007. Functional analysis of rice *NPR1*-like genes reveals that *OsNPR1*/*NH1* is the rice orthologue conferring disease resistance with enhanced herbivore susceptibility. Plant Biotechnol. J. 5:313-324.

Zhang, X., Yao, X., Qin, C., Luo, P., and Zhang, J. 2016. Investigation of the molecular mechanisms underlying metastasis in prostate cancer by gene expression profiling. Exp. Ther. Med. 12:925-932.

Zhao, S., Wu, Y., and Wu, J. 2021. Arms race between rice and viruses: A review of viral and host factors. Curr. Opin. Virol. 47:38-44.